

Article

Study of Aeration and CO₂ Absorption Using Filtration Membranes in Terms of Physical Properties and Mass Transfer Parameters

Kasidit Phanpa^{1,a}, Kritchart Wongwailikhit^{1,b*}, Rawadee Dammee¹, Sermpong Sairiam², Marupatch Jammongwong³, and Pisut Painmanakul¹

¹ Department of Environmental Engineering, Faculty of Engineering, Chulalongkorn University, Bangkok 10330, Thailand

² Department of Science, Chulalongkorn University, Bangkok 10330, Thailand

³ Department of Civil Engineering, King Mongkut's University of Technology North Bangkok, Bangkok 10800, Thailand

E-mail: ^akasidit.ph@student.chula.ac.th, ^bkritchart@hotmail.com (Corresponding author)

Abstract. Hollow fiber membrane contactor is nowadays one of the alternative absorption processes for the conventional bubble column. In this work, the performances of microporous hollow fiber membranes for aeration and CO₂ absorption were investigated and compared with a conventional bubble column. The membranes used in this work were adapted from filtration membranes which are significantly cheaper than conventional absorption membranes. The effects of operating variables such as average pore sizes, gas flow rates, liquid flow rates, number of hollow fiber membrane, and concentrations of chemical solution on the gas-liquid absorption rate were determined. For oxygen-water absorption, the overall mass transfer coefficient ($k_{L,a}$), which corresponding to the absorption rate, increased with the increase of membrane porous diameter. The $k_{L,a}$ was also enhanced with the increase of the liquid flow rate and the number of membranes while the gas flow rate was rarely influent. For carbon dioxide absorption, the increase in liquid flow rate and the carbon dioxide concentration resulted in higher mass transfer rate. Moreover, adding sodium carbonate in absorbent improved the $k_{L,a}$ value up to 2.2 folds, comparing with physical absorption. The comparison between the membrane contractor and a bubble column indicated that the utilization of filtration membranes had more efficiency comparing to bubble column due to its high surface area and adaptability when operating with the same size especially when using lower gas velocity rate.

Keywords: Gas absorption, hollow fiber membrane contactors, aeration, CO₂ absorption, filtration membranes.

ENGINEERING JOURNAL Volume 22 Issue 4

Received 29 October 2017

Accepted 9 April 2018

Published 31 July 2018

Online at <http://www.engj.org/>

DOI:10.4186/ej.2018.22.4.83

1. Introduction

Carbon dioxide (CO₂) is, nowadays, one of the concerning substances for global warming. The concentration of CO₂ in atmospheric has dramatically increased to approximately 450 ppm by 2030 and between 750 ppm and 1,300 ppm by 2100 [1]; Increasing of CO₂ in atmospheric causes global warming, climate change, and subsequently affects creatures in earth. The major cause of the increase of CO₂ in atmosphere is the combustion of organic substances that used for energy generation, electricity, and industry processes. In order to prevent the exposing of CO₂, the conventional equipment for CO₂ absorption were pioneered including bubble column, spray column, packed column and tray column. All of the operations provide contacting areas between gas and liquid to transfer CO₂ from gas phase to liquid phase in order to reduce the amounts of CO₂ exposing to atmosphere. From all equipment, bubble column is widely used because of its ease in operation procedure, absorption capacity as well as its low operating cost. However, industrial-scale bubble columns are confronted a variety of operational problems including flooding, entrainment and foaming [2]. Hence, in this recent years, the gas absorption using hollow fiber membrane contactor has been investigated to be an alternative of the bubble column; not only it can provide greater gas-liquid transfer area comparing to the conventional equipment [3] but also its operational flexibility, economic operating cost, linear scale-up, and simple prediction [4].

The success of using hollow fiber membranes for CO₂ removal can be found in many researches. For CO₂-water absorption, various removal efficiencies were reached, depending on their operating conditions and material of membranes [5-9]. The maximum CO₂ removal of 76% by the absorption in water was achieved in a polypropylene hollow fiber membrane [5], while only 20% of CO₂ removal efficiency was reached with a polyvinylidene fluoride membrane [6]. The improvement of CO₂ removal could be done by introducing the chemical reaction that could enhance the treatment efficiency up to 87% when the monoethanolamine was used with a polypropylene membrane [7].

The membranes used in the membrane contactor can be hydrophobic or hydrophilic and its pores can be either gas filled or liquid filled [5, 10]. Hydrophobic surface membranes with high porosity and chemical resistance was claimed to be the most effective one [11]. It was also found that the throughput of liquid in the tube side offers a significant improvement in performance, comparing when operating in the shell side of the module [3]. Normally, specific absorption membranes are made of polypropylene (PP) and Polytetrafluoroethylene (PTFE). Regarding the hollow membrane required very specific characteristics (i.e. chemical resistance, high porosity etc.), the cost of production for these membranes are very high [11]. In order to overcome the problem, in this work, the membrane using for filtration process was adapted to use in absorption system since filtration membranes also have high porosity, chemical resistance with significantly lower cost.

Therefore, this research purpose was to investigate the performances of hollow fiber filtration membranes and compared their performance with conventional bubble column in term of the overall volumetric mass transfer coefficient ($k_{L,a}$). The specific design criteria and the suitable correlation for predicting the performance of hollow fiber membrane contactors for gas absorption of O₂ and CO₂ were identified.

2. Methodology

2.1. Membrane Characterization

In this research, a polyvinylidene fluoride microfiltration membrane (MF), represented as type A, and two Ultrafiltration membranes (UF), represented as type B and C, were studied. Their physical characteristics were identified with an environmental scanning electron microscope (ESEM). The Wilhelmy method was applied to measure the contact angle of the membranes surfaces [11].

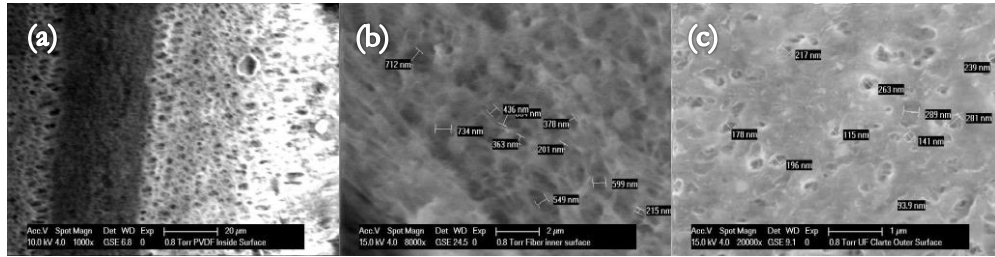


Fig. 1. Membrane surface morphology (a) Membrane A (b) Membrane B (c) Membrane C.

The structures and surfaces of membrane A, B and C identified with ESEM are illustrated as in Fig. 1. The surface of membrane A was smooth as can be seen in Fig. 1(a). The porous diameter of membrane A was $0.160\ \mu\text{m}$; the contact angle of membrane A was 61.1° which indicated that the surface of membrane A was hydrophilic. The membrane B and C consisted of fibers (Type B) and small porous (Type C), as shown in Fig. 1(b) and 1(c), had their porous diameter to 0.024 and $0.109\ \mu\text{m}$, respectively. The property of membrane B and C were hydrophobic and hydrophilic corresponding to their contact angle of 136.0 and 0.0 , respectively. The summary of the characteristics of hollow fiber membranes are provided in Table 1.

Table 1. Characteristics of hollow fiber membrane used in this research.

Type	Porous diameter (μm)	DCA ($^\circ$)	Hydro-property
A	0.160	61.1	Hydrophilic
B	0.024	136.0	Hydrophobic
C	0.109	0	Hydrophilic

2.2. Experimental Set-Up

In this work, both aeration and CO_2 absorption were studied. The equipment used in the aeration process were set up as illustrated in Fig. 2. The hollow fiber membranes were placed inside a 1-cm inside-diameter and 20-cm effective length glass module. Air was fed to the shell side of the glass module with air pump and regulated its flow rate with a flow meter. The air flew pass the outer surface of hollow fiber membrane before exposed to atmosphere. The inside of hollow fiber membranes were connected to liquid pump in order to circulate liquid inside membrane and liquid circulation system. The counter current regime was selected as it provided a great driving force for mass transfer [3]. Oxygen-free water was prepared by the chemical reaction of sodium sulphite (Na_2SO_3) with dissolved oxygen in water [12]. Within the liquid flow circulation line, a dissolved oxygen sensor, Horiba OM-51, was used to measure oxygen concentration in liquid phase as function of time.

For carbon dioxide experiments, experimental set-up was almost the same as aeration system exclude gas feeding system and the measurement methodology. Noted that for CO_2 absorption system, the gas phase was not continuously flow but accumulated within the shell side of module due to the limitation of measurement. The initial CO_2 concentration at 9000 ppm was prepared by mixing pure CO_2 with fresh air before initiated to the shell side of membrane. The Testo CO_2 -535 was used as the CO_2 concentration sensor inside the reactor in order to determine mass transfer parameters and its efficiency. The deionized water with sodium carbonate (Na_2CO_3) solution at 0, 1, 5, and 10 percent by weight was used as liquid phase for absorption of CO_2 .

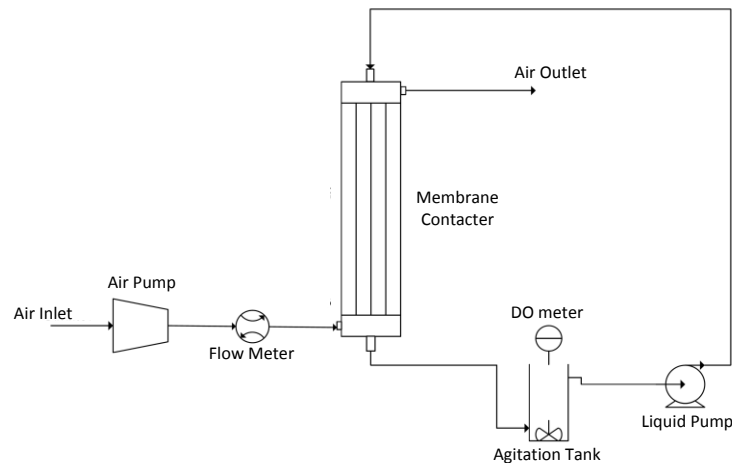


Fig. 2. Experimental set-up for aeration system.

2.3. Analytical Method

In all experiments, the concentration data was collected every 10 seconds until 30 minutes to ensure that the steady state had been reached. All the experiments were conducted at temperature of 25 °C.

2.3.1. Determination of overall mass transfer coefficient ($k_L a$) in aeration system

The mass transfer coefficient ($k_L a$) for aeration process (O_2 absorption in water) were determined by applying the American Society of Civil Engineers (ASCE) method [13] which derived from mass balance equation as shown in Eq.(1);

$$\frac{dC}{dt} = k_L a (C^* - C_L) \quad (1)$$

where its integration form is expressed as in Eq. (2)

$$\ln(C^* - C_L) = \ln(C^*) - k_L a \cdot t \quad (2)$$

From Eq. (2), $k_L a$ value was determined from the slope of $\ln(C^* - C_L)$ and t .

2.3.2. Determination of overall mass transfer coefficient ($k_L a$) in CO_2 absorption system

The $k_L a$ determination method for CO_2 absorption system was different from aeration system because the gas phase was not flow continuously. The method was initially derived with the mass balance equation of CO_2 transferred between gas and liquid phase. At any transfer concentration, the change of dissolved CO_2 in liquid phase must be equal to CO_2 transferred from gas phase. Hence, the CO_2 balance equation is given by the following Eq. (3) and can be written as in Eq. (4) where V refers to volume of fluid in system, C refers to CO_2 concentration, subscripts of g and L refer to gas and liquid phase while i and t are corresponding to initial and at considered time respectively.

$$\Delta C_g V_g = \Delta C_L V_L \quad (3)$$

$$(C_{g,in} - C_{g,t}) V_g = (C_{L,t} - C_{L,i}) V_L \quad (4)$$

As the initial CO_2 concentration in DI-water was zero, concentration of gas as function of liquid concentration can be expressed as in Eq. (5);

$$C_{g,t} = C_{g,in} - \frac{C_{L,t}V_L}{V_G} \quad (5)$$

Eq. (1) combines with Henry's Law can be written as;

$$\frac{dC}{dt} = k_L a (C^* - C_{L,t}) = k_L a (k_H C_{g,t} - C_{L,t}) \quad (6)$$

Combine Eq. (5) with Eq. (6) yields;

$$\frac{dC}{dt} = k_L a \left[k_H C_{g,in} - C_{L,t} \left(\frac{k_H V_L}{V_G} + 1 \right) \right] \quad (7)$$

Define $\theta = \frac{k_H V_L}{V_G} + 1$, therefore, Eq. (7) becomes;

$$\frac{1}{k_H C_{g,in} - C_{L,t} \theta} dC_{L,t} = k_L a \cdot dt \quad (8)$$

$$\ln \frac{k_H C_{g,in} - C_{L,t} \theta}{k_H C_{g,in} - C_{L,t} \theta} = -k_L a \cdot \theta \cdot t \quad (9)$$

From Eq. (9), the $k_L a$ for CO₂ absorption can be obtained from slope of $\ln \frac{k_H C_{g,in} - C_{L,t} \theta}{k_H C_{g,in} - C_{L,t} \theta}$ and θt .

2.3.3. CO₂ Removal efficiency

CO₂ removal efficiency is considered from difference between CO₂ concentration at initial condition and at considered time with initial concentration as divisor as shown in Eq. (10)

$$\text{CO}_2 \text{ Removal Efficiency} = \frac{\text{CO}_{2,\text{initial}} - \text{CO}_{2,\text{at time } t}}{\text{CO}_{2,\text{initial}}} \times 100 \% \quad (10)$$

3. Results and Discussions

3.1. Membrane Selection

The oxygen-water absorption experiment was conducted at gas and liquid flow rate of 10 LPM and 0.1 LPM respectively. The results as shown in Fig. 3 indicated that the $k_L a$ of membrane A were higher than B and C due to its larger porous size. However, membrane B that had smaller porous diameter yielded higher $k_L a$ than membrane C; it was possibly happened because the surface of membrane B was hydrophobic which normally dry during the operation between air and water. This dry operation was confirmed to achieve higher rate comparing with the wet operation of hydrophilic surface [14]. According to its highest mass transfer coefficient, membrane A was selected to study the effect of operating conditions on its mass transfer parameters and efficiency.

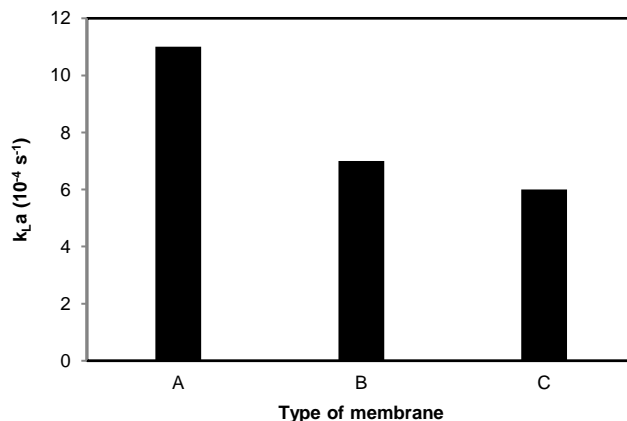


Fig. 3. Comparison of the $k_{L,a}$ in aeration system with different types of membrane. ($Q_g = 10$ LPM, $Q_L = 0.1$ LPM, Number of membrane module = 5).

3.2. Effect of Operating Variables and Membrane Configuration on the Overall Mass Transfer Coefficient ($k_{L,a}$)

In this part, the effect of operating variables consisted of gas flow rate, liquid flow rate as well as number of membrane on overall mass transfer coefficient ($k_{L,a}$) of membrane A were investigated.

3.2.1. Effect of gas flow rate

Figure 4 illustrates the effect of gas flow rate on the $k_{L,a}$ at constant liquid flow rate of 0.1 l/min. In the figure, the $k_{L,a}$ value slightly rose as the gas flow rate included which implied that the gas flow rate had slightly effect on the $k_{L,a}$. Due to this fact, it could be interpreted that the mass transfer rate for the hollow fiber membrane was limiting at liquid interphase [6, 15].

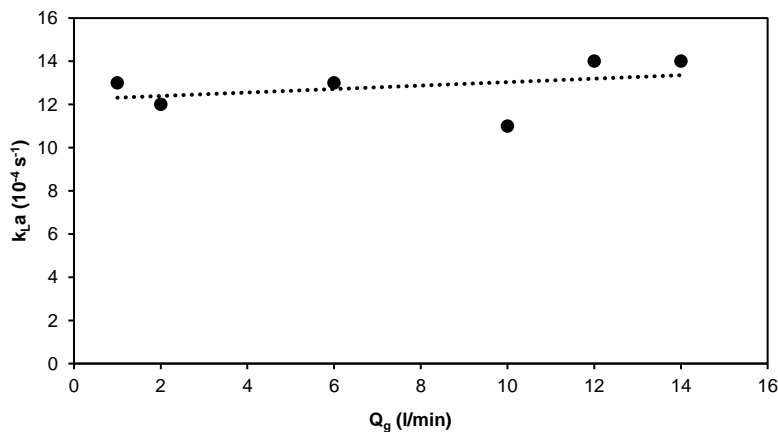


Fig. 4. Effect of the gas flow rate on the overall mass transfer coefficient ($k_{L,a}$) in aeration system ($Q_L = 0.1$ LPM, Number of membrane module = 5).

Similar results were reported by Wang et al. [15], the gas flow rate was found to have no impact on the overall mass transfer coefficient. Not only for the aeration process, it was also confirmed by Atchariyawut et al [6] that the mass transfer resistance of CO_2 -water absorption was limiting in the liquid phase, which normally found in the absorption of low-soluble substances.

3.2.2. Effect of liquid flow rate

Figure 5 shows the effect of liquid flow rate on the $k_{L,a}$ at gas flow rate of 2 l/min. As seen in the figure, the increasing in liquid flow rate greatly enhanced $k_{L,a}$ value especially at low liquid flow rate. The increment of liquid flow rate caused higher liquid velocity in the hollow membrane, and reduced the mass transfer resistance in liquid phase. The observation is supported by Graetz-Lévêque equation (Eq. 11) which normally used to predict the tube side mass transfer coefficient [16, 17].

$$\text{Sh} = \frac{k_L d_i}{D_i} = 1.62 \sqrt[3]{\frac{d_i^2 V_L}{L \cdot D_i}} \quad (11)$$

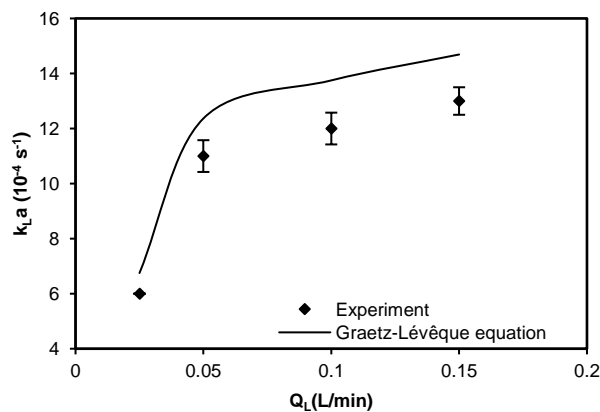


Fig. 5. Effect of the liquid flow rate on the overall mass transfer coefficient ($k_{L,a}$) in aeration system ($Q_g = 2$ l/min, Number of membrane module = 5).

The similar behavior was also reported by Wang et al. [15]. It was claimed that the increase of the liquid velocity could accelerate the supply of the active absorbent, increase mixing, and mitigate the depletion effectively. As the result, the gas absorption flux increased with the increase of the liquid velocity. Fortescue et.al [18] and Atcharyawut et al [6] also mentioned this similar effect in term of Reynolds number.

3.2.3. Effect of the amount of hollow fiber membrane

The effect of the amount of hollow fiber membrane is presented in Fig. 6. The result obviously indicated that the $k_{L,a}$ roughly increased equal to the increase of the total amounts of membrane used. As can be seen in the figure, applying 5 units approximately provided the $k_{L,a}$ at $11 \times 10^{-4} \text{ s}^{-1}$ while applying 10 units yield the $k_{L,a}$ at around $21 \times 10^{-4} \text{ s}^{-1}$ which was approximately two times higher. It could be clearly explained that, since the overall mass transfer coefficient ($k_{L,a}$) consists with two terms in multiply i.e. liquid side mass transfer coefficient (k_L) and specific interfacial area (a), the increment of unit numbers of membrane significantly increased the interfacial area (a) equals to the times of unit increase and, consequently, rose the $k_{L,a}$ [19].

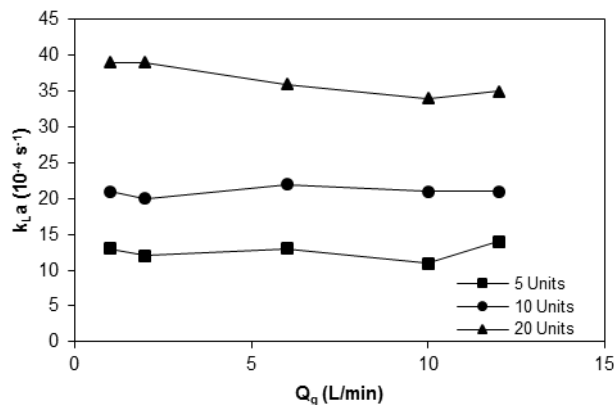


Fig. 6. Effect of number of hollow fiber membrane on the overall mass transfer coefficient ($k_{L,a}$) in aeration system ($Q_L = 0.1$ l/min).

3.3. Comparison the $k_{L,a}$ between Hollow Fiber Membrane Contactor and Bubble Column Reactor

The comparison of the bubble column results of Sastaravet et al. [20] with the $k_{L,a}$ from membrane type A is depicted in Fig. 7. According to their bubble column, three types of single orifices including flexible (Fo1), rigid (R1), and flexible orifice (F1) were used in a cylindrical bubble column with 5 cm diameter and 30 cm height. From their experiments, the $k_{L,a}$ were clearly affected by the gas velocity (V_g) in the bubble column which was contrasted with the results of the membrane reactor. The $k_{L,a}$ of the membrane system was superior especially at the low gas velocity with 20 units of membranes. As mentioned earlier, the significant parameter affected $k_{L,a}$ of membrane system was the numbers of unit membrane module while the control variable for the bubble column was superficial velocity which was not flexible. The increase of the amounts of membranes would intensely rise the $k_{L,a}$ to above the conventional bubble column; the modification was easier comparing to the adaption of gas velocity in bubble columns. Hence, this membrane contactor had an advantage to bubble column not only in term of its adaptability but also its mass transfer performance.

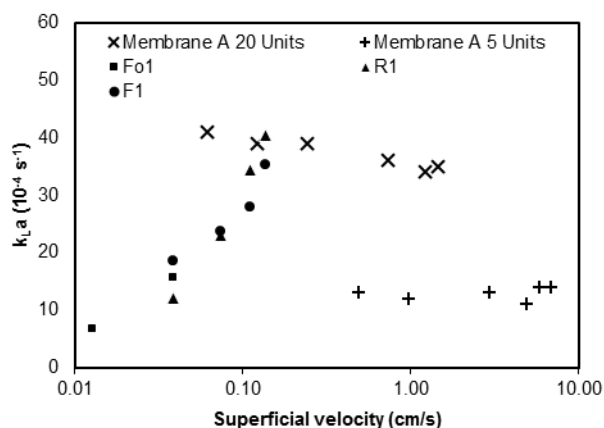


Fig. 7. Comparison of the $k_{L,a}$ between the membrane contactor and the cylindrical bubble column [20] in the different gas superficial velocity.

3.4. The Empirical Correlation for Aeration Process of the Hollow Fiber Membrane

The previous part indicated that the $k_{L,a}$ from membrane contactor was the function of the liquid volumetric flow rate, the numbers of membrane tube and the surface type of membrane described by the contact angle (θ). With the purpose of further usage and design, the correlation between these variables was developed in term of dimensionless groups since it has an advantage in representing the system phenomena. With this purpose, the Buckingham Pi theorem was applied [21]. The dependent variable for the system was the $k_{L,a}$

while the independent variables were liquid density (ρ_L), liquid viscosity (μ_L), membrane outside diameter (d_o), liquid velocity in membrane (V_L), contact angle of surface membrane (θ), numbers of membrane in system (n) and inside diameter of module (D_i). After the Buckingham Pi Theorem was applied the relationship of variables can be described as in Eq. (12).

$$\frac{k_L a V_L}{g} = f(\text{Re}_L, \phi, \theta) \quad (12)$$

In the equation, the $k_L a$ is formed the dimensionless group with V_L and g and is the function of liquid Reynolds number (Re_L), packing density (ϕ) and contact angle of membrane surface (θ). The liquid Reynolds number and packing density are expressed in Eq. (13) and (14), respectively.

$$\text{Re}_L = \frac{\rho_L V_L d_i}{\mu_L} \quad (13)$$

$$\phi = n \left(\frac{d_o}{D_i} \right)^2 \quad (14)$$

The non-linear regression was applied to obtain the relations between each group and found that the relation was in form of exponential as showed in Eq. (15). Each parameter of the equation is expressed in Eq. (16)-(18).

$$\frac{k_L a V_L}{g} = K \text{Re}_L^a \phi^b \quad (15)$$

where;

$$K = 2.68 \times 10^{-10} [3,500 - 111(\theta) + (\theta)^2] \quad (16)$$

$$a = 1.29 + 0.0069(\theta) - 5.2 \times 10^{-5} (\theta)^2 \quad (17)$$

$$b = 2.45 - 0.033(\theta) + 2.21 \times 10^{-4} (\theta)^2 \quad (18)$$

From Eq. (15), the mass transfer coefficient dimensionless group is majorly depending on the liquid Reynold number and packing density as both variables were in exponential function to it. However, the contact angle plays an important role as it affects all parameters in Eq. (15) in form of parabolic function, Eq. (16)-(18). The optimum contact angle for the aeration process predicting with Eq. (15) is 98 degrees which is the hydrophobic surface membrane that was claimed to be better than hydrophilic [14]. For validation, this model accuracy was identified by comparing the calculated values from Eq. (15) and the experimental values at the same condition as depicted in Fig. 8. The figure indicates that the $k_L a$ value from the equation are consistent with the experimental results with the average deviation than ± 13.26 %.

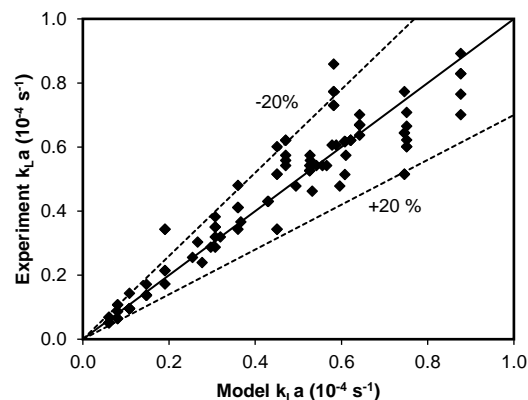


Fig. 8. Comparison of $k_{L,a}$ from the experiment and the empirical correlation for aeration in hollow fiber membrane.

3.5. Application of Hollow Fiber Membrane: CO₂ Absorption

In this part, the $k_{L,a}$ for CO₂ absorption and CO₂ removal efficiency were studied. The liquid phase was constantly circulated at 0.15 l/min for all the CO₂ experiment.

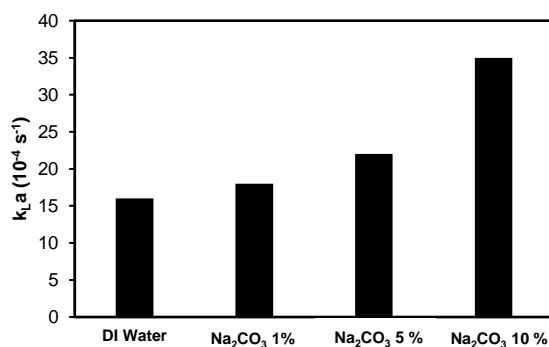


Fig. 9. Comparison of $k_{L,a}$ between physical and chemical absorption.

Figure 9 illustrates the results of CO₂ absorption in different Na₂CO₃ concentration. The increase of Na₂CO₃ concentration rose the $k_{L,a}$ value since CO₂ is the acid gas which can rapidly react with base solution of Na₂CO₃. Therefore, as can be seen in Fig. 10 which compares the CO₂ removal efficiency between at different concentrations of Na₂CO₃ for time up to 30 minutes, the treatment efficiency of CO₂ rose rapidly at time between 0-10 minutes especially for higher concentration of Na₂CO₃. The treatment efficiency subsequently went up slowly to approximate 80 percent for any concentration of Na₂CO₃ and 62 percent for DI water. For time between 0-3 minute, the higher concentration of Na₂CO₃ resulted in faster reaction and higher $k_{L,a}$; the treatment efficiency for higher concentration was higher over this period. However, after 3 minute, the different of Na₂CO₃ concentration didn't have clearly effect on the treatment efficiency despite of their $k_{L,a}$ value. This occurred due to the decrease of saturated concentration CO₂ when presenting of Na₂CO₃ particularly at high concentration [22]. The decrease of CO₂ saturated concentration reduced the mass transfer rate as C_L^* in Eq. (1) was decreased.

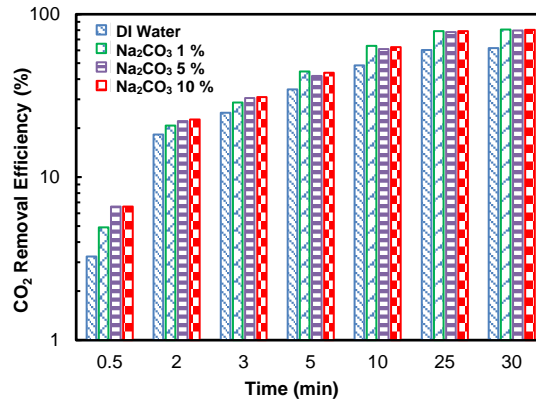


Fig. 10. Comparison of CO₂ removal efficiency between physical and chemical absorption.

Moreover, the prediction model for CO₂ absorption was developed following the methodology of the aeration empirical model. From the non-linear regression, the prediction equation for CO₂ absorption was found to be in term of exponential function with liquid Reynolds number (Re_L) and initial gas concentration ($C_{g,initial}$). The chemical absorption was also concerned by addition of Na₂CO₃ concentration term as expressed in Eq. (16). The accuracy of this equation is very satisfactory with the deviation less than $\pm 3.77\%$ as depicted in Fig. 11.

$$\frac{k_L a V_L}{g} = 1.03 \times 10^{-11} C_{g,initial}^{0.92} Re_L^{1.26} + 4.21 \times 10^{-6} C_{Na_2CO_3} \quad (16)$$

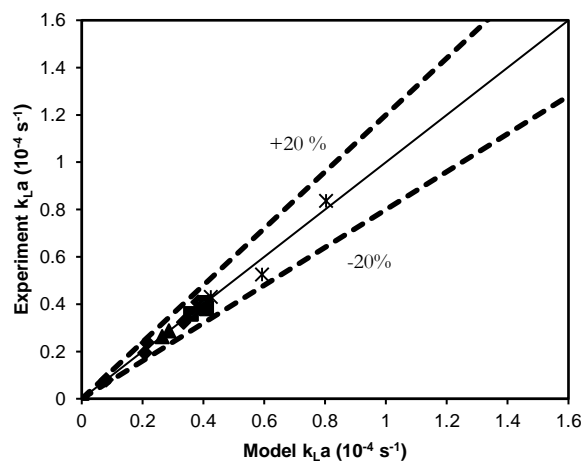


Fig. 11. Comparison of $k_L a$ from the experiment and the empirical correlation for CO₂ absorption in hollow fiber membrane.

4. Conclusion

This research investigated the overall mass transfer coefficient ($k_L a$) for three different types of microporous hollow fiber membrane which normally used in filtration process. These types of membranes are cheaper than the conventional membrane used in the absorption process. It was found that these membranes could be used for the aeration process and absorption of CO₂ effortlessly. The membranes also had an advantage over a bubble column as it could increase its mass transfer rate flexibly by increasing the number of membranes that resulted in rising its interfacial area significantly. Moreover, the effects of each operating parameter were determined. The consistent results with the commercial absorption membrane were obtained. For the same number of membrane tube, the membrane with the largest porous diameter yielded the highest $k_L a$ value since it provided greater contact area. The contact angle also played an important role regarding

their operating surfaces. The hydrophobic surface trended to have higher $k_{L,a}$ value for aeration process since the operating surface was dry when operating with water. The $k_{L,a}$ value was also affected with the increase of the liquid flow rate but rarely affected on the gas flow rate because the mass transfer rate was limiting at the liquid phase. The membrane could also applied to absorb CO_2 gas into liquid phase. It was confirmed that the carbon dioxide treatment efficiency up to approximate 80 percent could be reached within 25 minute with the assistance of Na_2CO_3 base solution. The empirical equations for prediction of the mass transfer coefficient for both aeration and CO_2 absorption were proposed with the acceptable accuracy.

Nomenclature

a	Specific Interfacial Area (m^{-1})
c_L	Dissolved Oxygen Concentration Saturation at Specific Time (mg/l)
c^*	Maximum Dissolved Oxygen Concentration Saturation (mg/l)
$c_{g,\text{initial}}$	Initial Gas Concentration (mg/l)
$c_{g,t}$	Gas Concentration at Specific Time (mg/l)
d_i	Inside Diameter of Hollow Fiber Membrane (m)
d_o	Outside Diameter of Hollow Fiber Membrane (m)
D_i	Inside Diameter of Module (m)
D_{iL}	The Diffusion Coefficient (m^2/s)
ESEM	Environment Scanning Electron Microscope
g	Gravitational Acceleration (m/s^2)
k_H	Henry 's Law Constant ($\text{L}\cdot\text{atm}/\text{mol}$)
$k_{L,a}$	Overall Mass Transfer Coefficient ($1/\text{s}$)
k_L	Liquid-Side Mass Transfer Coefficient (m/s)
L	Effective Length of The Membrane Module (m)
n	Number of Hollow Fiber Membrane
Q_g	Gas Flow Rate (l/min)
Q_l	Liquid Flow Rate (l/min)
Re	Reynolds Number
Sh	Sherwood Number
t	Time (s)
V_g	Gas Velocity (m/s)
V_l	Liquid Velocity (m/s)
Greek letters	
ρ_l	Liquid Density (kg/m^3)
μ_l	Viscosity of Liquid ($\text{Pa}\cdot\text{s}$)
\emptyset	Membrane Module Packing Density
θ	Contact Angle of Membrane Surface ($^\circ$)

Acknowledgement

This research was funded by the Graduate School Thesis Grant, the Ratchadapisek Sompoch Endowment Fund (2016) CU-59-052-CC, Chulalongkorn University and Climate Change and Disaster Management Cluster.

References

- [1] M. R. Henderson, A. S. Reinert, P. Dekhtyar, and A. Migdal, "Climate change in 2017: Implications for business," Harvard Business School, 317-032, 2017.
- [2] W. Rongwong, S. Boributh, S. Assabumrungrat, N. Laosiripojana, and R. Jiratananon, "Simultaneous absorption of CO_2 and H_2S from biogas by capillary membrane contactor," *Journal of Membrane Science*, vol. 392–393, pp. 38–47, 2012.
- [3] D. deMontigny, P. Tontiwachwuthikul, and A. Chakma, "Using polypropylene and polytetrafluoroethylene membranes in a membrane contactor for CO_2 absorption," *Journal of Membrane Science*, vol. 277, pp. 99–107, 2006.

- [4] J. Lia and B. H. Chen, "Review of CO₂ absorption using chemical solvents in hollow fiber membrane contactors," *Separation and Purification Technology*, vol. 41, pp. 109–122, 2005.
- [5] S. Karoor and K. K. Sirkar, "Gas absorption studies in microporous hollow fiber membrane modules," *Industrial & Engineering Chemistry Research*, vol. 32, pp. 674–681, 1993.
- [6] S. Atcharyawut, R. Jiratananon, and R. Wang, "Separation of CO₂ from CH₄ by using gas–liquid membrane contacting process," *Journal of Membrane Science*, vol. 304, pp. 163–172, 2007.
- [7] L. Zhang, B. Hu, H. Wu, X. Wang, R. Liu, and L. Yang, "CO₂ Capture Using Hollow Fiber Membrane Under Wet Ammonia-Based Desulfurization Flue Gas Conditions," in *Clean Coal Technology and Sustainable Development*. Springer Singapore, 2016.
- [8] M. Sandru, S. H. Haukebo, and M. B. Hägg, "Composite hollow fiber membranes for CO₂ capture," *Journal of Membrane Science*, vol. 346, pp. 172–186, 2010.
- [9] F. Porcheron, D. Ferré, E. Favre, P. T. Nguyen, O. Lorain, R. Mercier, and L. Rougeau, "Hollow fiber membrane contactors for CO₂ capture: from lab-scale screening to pilot-plant module conception," *Energy Procedia*, vol. 4, pp. 763–770, 2011.
- [10] S. Khaisri, D. deMontigny, P. Tontiwachwuthikul, and R. Jiratananon, "A mathematical model for gas absorption membrane contactors that studies the effect of partially wetted membranes," *Journal of Membrane Science*, vol. 347, no. 228–239, 2010.
- [11] S. Sairiam, "Ozonation of dye wastewater by membrane contacting process using modified PVDF membranes," Doctor's Thesis, Department of Science, Chulalongkorn University, 2013.
- [12] The Dow Chemical Company, "The removal of oxygen and chlorine from water," Tech Facts, May 2002.
- [13] *Measurement of oxygen transfer in clean water*, ASCE Standard, 2nd ed, 1992.
- [14] W. Rongwong, R. Jiratananon, and S. Atcharyawut, "Experimental study on membrane wetting in gas–liquid membrane contacting process for CO₂ absorption by single and mixed absorbents," *Separation and Purification Technology*, vol. 69, pp. 118–125, 2009.
- [15] R. Wang, H. Y. Zhang, P. H. M. Feron, and D. T. Liang, "Influence of membrane wetting on CO₂ capture in microporous hollow fiber membrane contactors," *Separation and Purification Technology*, vol. 46, pp. 33–40, 2005.
- [16] A. Gabelman and S. Hwang, "Hollow fiber membrane contactors," *Journal of Membrane Science*, vol. 159, pp. 61–106, 1999.
- [17] M. C. Yang and E. L. Cussler, "Designing hollow-fiber contactors," *AIChE Journal*, vol. 32, no. 11, pp. 1910–1916, 1986.
- [18] G. E. Fortescue and J. R. A. Pearson, "On gas absorption into a turbulent liquid," *Chemical Engineering Science*, vol. 22, pp. 1163–1176, 1967.
- [19] J. Wu and V. Chen, "Shell-side mass transfer performance of randomly packed hollow fiber modules," *Journal of Membrane Science*, vol. 172, pp. 59–74, 2000.
- [20] P. Sastaravet, C. Chuenchaem, N. Thaphet, N. Chawaloeshonsiya, and P. Painmanakul, "Comparative study of mass transfer and bubble hydrodynamic parameters in bubble column reactor: physical configurations and operating conditions," *Environmental Engineering Research*, vol. 19, no. 4, pp. 345–354, 2014.
- [21] E. Bormashenko, "Generalization of the Buckingham Pi-Theorem," Ariel University, Natural Science Faculty, Physical Department, 2016.
- [22] B. P. Spigarelli, "A novel approach to carbon dioxide capture and storage," Doctoral Thesis, Department of Chemical Engineering. Michigan Technological University, 2013.